ITERATIVE LEARNING CONTROL APPLICATION TO A 3D CRANE SYSTEM

Radu-Emil Precup, Florin-Cristian Enache, Mircea-Bogdan Rădac
Dept. of Automation and Appl. Inf., "Politehnica" University of Timisoara, Bd. V. Parvan 2, 300223 Timisoara, Romania

Emil M. Petriu
School of Information Technology and Eng., University of Ottawa, 800 King Edward, Ottawa, ON, K1N 6N5, Canada

Claudia-Adina Dragoş, Stefan Preitl
Dept. of Automation and Appl. Inf., "Politehnica" University of Timisoara, Bd. V. Parvan 2, 300223 Timisoara, Romania

Keywords: 3D crane system, Cascade Learning, Design approach, Iterative Learning Control.

Abstract: This paper deals with the application of an Iterative Learning Control (ILC) structure to the position control of a 3D crane system in the crane position control problem. The control system structure involves Cascade Learning (CL) built around control a loop with a frequency domain designed lead-lag controller. The parameters of the continuous-time real PD learning rule as lead-lag controller are set such that to fulfil the convergence condition of the CL process. A set of real-time experimental results concerning a 3D crane system laboratory equipment is offered to validate the new CL-based ILC structure.

1 INTRODUCTION

The gantry crane systems are important in many industrial applications including the 3D crane systems as representative Multi Input-Multi Output (MIMO) systems. Some current control approaches related to 3D crane systems reported in the literature deal with the combination of time-optimal control and of visual feedback (Yoshida and Tabata, 2008), PID controllers with friction compensation (Westerberg et al., 2008), inertia theorem-based nonlinear controllers (Chang and Chiang, 2008), nonlinear tracking control structures (Chwa, 2009), feed-forward and input-shaping techniques (Kaneshige et al., 2009), sliding mode control (Pisano et al., 2010) or gain scheduling techniques (Cuenca et al., 2011).

Iterative Learning Control (ILC) is based on the fact that the performance indices (overshoot, settling time, etc.) of control systems executing repetitively the same tasks can be improved using previous experiments, referred to also as cycles or iterations, in the control system operation. Several learning rules are implemented in ILC structures that are built around the control system whose performance is improved (Bristow et al., 2006; Ahn et al., 2007; Xu et al., 2009).

This paper gives a new solution to the crane position control problem dedicated to a 3D crane system laboratory equipment that models industrial gantry crane systems (Inteco, 2008). Our control system structure involves Cascade Learning (CL) (Xu et al., 2009) built around a control loop with a frequency domain designed lead-lag controller. The parameters of the continuous-time real PD learning rule as lead-lag controller are set such that to fulfil the convergence condition of the learning process in the CL-based control system structure. The convergence condition guaranteed by our ILC structure is an inequality that employs a frequency domain calculated H_∞ norm.

This paper suggests two contributions with this regard. First, a new control system structure based on the combination of lead-lag control and ILC is suggested. Second, real-time experimental results are included to validate our new control system structure.

Precup R., Enache F., Rădac M., Petriu E., Dragoş C. and Preitl S..
ITERATIVE LEARNING CONTROL APPLICATION TO A 3D CRANE SYSTEM.
DOI: 10.5220/0003537301170122
In *Proceedings of the 8th International Conference on Informatics in Control, Automation and Robotics* (ICINCO-2011), pages 117-122
ISBN: 978-989-8425-74-4

The two contributions of this paper are important and also advantageous with respect to the current literature in the field because they ensure the simple design of both the lead-lag controller and the learning rule. Frequency domain approaches are used in this context.

This paper is structured as follows. The process models are presented in the next section. Section 3 focuses on the design of the new control system structure. A set of real-time experimental results is given in Section 4 to validate the new CL-based ILC structure. The conclusions are given in Section 5.

2 PROCESS MODELS

It is accepted that the state variables of the MIMO state-space model of the process are (Chen et al., 2008; Inteco, 2008) x_1 – the distance of the cart from the centre of the rail, x_{10} – the initial condition for x_1, x_2 – the speed of the cart on the direction of x_1, x_3 – the distance of the rail with the cart from the centre of the construction frame, x_4 – the speed of the rail with the cart on the direction of x_3, x_5 – the acute angle between the lift-line of the payload and the rail, x_6 – the angular speed that corresponds to x_5, x_7 – the acute angle between the lift-line of the payload and the vertical line, x_8 – the angular speed that corresponds to x_7, x_9 – the length of the lift-line, and x_{10} – the speed of the lift-line.

The control signals in the process model are u_1, u_2 and u_3 that correspond to the PWM duty cycles applied to the DC motors that actuate the system on the axes x_1, x_3 and x_9, respectively. The three axes x_1, x_3 and x_9 are referred to as follows the x-axis, the y-axis, and the z-axis, respectively.

The nonlinear state-space equations of the process in the 3D crane system are expressed in (1) if no disturbance are considered and zero initial conditions are considered for all state variables excepting x_1 by the transformation of the equations given in (Chen et al., 2008; Inteco, 2008).

Therefore the MIMO state-space model of the process and the parameter values, obtained from the first-principle model of the process, are given as follows in (1) and (2), respectively:

$$
\begin{aligned}
&\dot{x}_1 = x_2,\\
&\dot{x}_2 = -T_1 x_2 - T_{sy}\,\mathrm{sgn}(x_2) - \mu_1 \cos(x_5)[-T_3 x_{10}\\
&- T_{sz}\,\mathrm{sgn}(x_{10})] + k_1 u_1 + k_3 \mu_1 \cos(x_5) u_3,\\
&\dot{x}_3 = x_4,\\
&\dot{x}_4 = -T_2 x_4 - T_{sx}\,\mathrm{sgn}(x_4) - \mu_2 \sin(x_5)\sin(x_7)\\
&\cdot[-T_3 x_{10} - T_{sz}\,\mathrm{sgn}(x_{10})] + k_2 u_2 + k_3 \mu_2 \sin(x_5)\\
&\cdot \sin(x_7) u_3,\\
&\dot{x}_5 = x_6,\\
&\dot{x}_6 = -[T_1 x_2 - T_{sy}\,\mathrm{sgn}(x_2)]\sin(x_5)/x_9 + \sin(x_3)\\
&\cdot \cos(x_5) x_8^2 / x_9 + \cos(x_5)\cos(x_7)[k_1 \sin(x_5) u_1\\
&- k_2 \cos(x_5)\sin(x_7) u_2 - k_3 \mu_2 \sin(x_5)\cos(x_5)\\
&\cdot \sin^2(x_7) u_3 + k_3 \mu_1 \sin(x_5)\cos(x_5) u_3]/x_9^2 + \mu_2\\
&\cdot \sin(x_5)\cos(x_5)\sin^2(x_7)[-T_3 x_{10} - T_{sz}\,\mathrm{sgn}(x_{10})]\\
&/ x_9 + \cos(x_5)\sin(x_7)[T_2 x_4 + T_{sx}\,\mathrm{sgn}(x_4)]/x_9\\
&- \mu_1 \sin(x_5)\cos(x_5)[-T_3 x_{10} - T_{sz}\,\mathrm{sgn}(x_{10})]/x_9\\
&- 2x_6 x_{10}/x_9,\\
&\dot{x}_7 = x_8,\\
&\dot{x}_8 = k_2 \sin(x_7)\cos(x_7) u_2 /[x_9^2 \sin^2(x_5)] - k_3 \mu_1\\
&\cdot \mu_2 \sin^2(x_7)\cos(x_7) u_3 /[x_9^2 \sin(x_5)] + \mu_2\\
&\cdot \sin(x_7)\cos(x_7)[-T_3 x_{10} - T_{sz}\,\mathrm{sgn}(x_{10})]/x_9 - 2x_8\\
&\cdot x_{10}/x_9 + \cos(x_7)[T_2 x_4 + T_{sx}\,\mathrm{sgn}(x_4)]\\
&/[x_9 \sin(x_5)],\\
&\dot{x}_9 = x_{10},\\
&\dot{x}_{10} = \cos(x_5)[T_1 x_2 + T_{sy}\,\mathrm{sgn}(x_2)] + x_8^2 x_9\\
&\cdot \sin^2(x_5) - k_1 \sin(x_5)\cos(x_5)\cos(x_7) u_1 - k_2\\
&\cdot \sin^2(x_5)\sin(x_7)\cos(x_7) u_2 + k_3 \sin(x_5)\\
&\cdot \cos(x_7)[-\mu_2 \sin^2(x_5)\sin^2(x_7) - \mu_1 \cos^2(x_5)\\
&- 1] u_3 + \mu_2 \sin^2(x_5)\sin^2(x_7)[-T_3 x_{10} - T_{sz}\\
&\cdot \mathrm{sgn}(x_{10})] + \sin(x_5)\sin(x_7)[T_2 x_4 + T_{sx}\,\mathrm{sgn}(x_4)]\\
&+ \mu_1[-T_3 x_{10} - T_{sz}\,\mathrm{sgn}(x_{10})] + \mu_1 \sin^2(x_5)[-T_3\\
&\cdot x_{10} - T_{sz}\,\mathrm{sgn}(x_{10})] + x_6^2 x_9 - T_3 x_{10} - T_{sz}\,\mathrm{sgn}(x_{10}),
\end{aligned}
\tag{1}
$$

$$
\begin{aligned}
&\mu_1 = 0.4156,\ \mu_2 = 0.1431,\ k_1 = 49.8636,\\
&k_2 = 16.0336,\ k_3 = -129.8258,\\
&T_1 = 11.5242,\ T_2 = 26.3263,\\
&T_3 = 217.3535,\ T_{sx} = 1.4903,\ T_{sy} = 6.4935,\\
&T_{sz} = 20.8333.
\end{aligned}
\tag{2}
$$

The controlled output, y, can be one or more of the state variables x_1, x_3, x_5, x_7 and x_9, and the

choice of the state variables depends on the control problem that is solved. The state variables x_1, x_3 are involved as controlled outputs in the crane position control problem, and the state variables x_5, x_7 and x_9 are involved as outputs in the anti-swing control problem. With this regard the process with the state-space equations given in (1) is a nonlinear MIMO system.

Several approaches can be used to simplify the nonlinear process model presented in (1) and (2). The strongest simplification is based on accepting that only the forces on the three axes x_1, x_3 and x_9 affect the movement of the system. The zero initial conditions result in the definition of the three transfer functions $H_x(s)$, $H_y(s)$ and $H_z(s)$:

$$\begin{aligned} H_x(s) &= x_1(s)/u_1(s) = k_x/[s(1+T_x s)], \\ H_y(s) &= x_3(s)/u_2(s) = k_y/[s(1+T_y s)], \\ H_z(s) &= x_9(s)/u_3(s) = k_z/[s(1+T_z s)], \end{aligned} \tag{3}$$

where k_x, k_y and k_z are the process gains, and T_x, T_y and T_z are the process time constants. The least-squares identification based on real-world input-output data measured from the laboratory equipment leads to the following parameter values (Enache, 2010):

$$\begin{aligned} k_x &= 0.2939, T_x = 0.0587\,\text{s}, \\ k_y &= 0.2747, T_y = 0.0379\,\text{s}, \\ k_z &= 0.1019, T_z = 0.0408\,\text{s}. \end{aligned} \tag{4}$$

The three transfer functions defined in (3) (with the parameters in (4)) can be viewed as three Single Input-Single Output (SISO) processes. Three SISO control loops can be designed, but the control systems design should account for the model simplification and for the interactions between the three control loops. The effects of these interactions cannot be neglected when control structures for x_9 are designed.

The ILC-based control system structure designed in the next section is dedicated to the x-axis and to the y-axis, i.e., it controls x_1 and x_3, respectively, using the process transfer functions $H_x(s)$ and $H_y(s)$. However, the experimental results to be presented in Section 4 were conducted for the real-world process.

3 CONTROL SYSTEM STRUCTURE

The ILC-based control system structure with CL is are presented in Figure 1, where r is the reference input, y is the controlled output, $e = r - y$ is the control error, u is the control signal, M is the memory block, the subscript j indicates the cycle (experiment) index, C and C_1 are the transfer functions of the controllers with the argument omitted for simplicity, and P is the process transfer function. The current control loop is characterized by the controller with the transfer function C, the reference input r_j and the index $j+1$. The controller with the transfer function C_1 is referred to also as the learning rule. The disturbance inputs are not included in Figure 1 as in many situations they are not repetitive. That is the reason why they were not applied in the real-time experiments.

If the error at the first cycle e_0 is finite and nonzero, $e_0 \in R \setminus \{0\}$, the convergence condition for the learning process in the ILC-based control system structure is

$$\left\| \frac{e_{i+1}}{e_i} \right\|_\infty \le \gamma \;\; \forall i \in N,\; 0 < \gamma < 1, \tag{5}$$

where the parameter γ determines the convergence speed, and the following general notation and frequency domain calculation are used for the H_∞ norm

$$\|G\|_\infty = \sup_{\omega \in \Omega} |G(j\omega)|, \tag{6}$$

with $j^2 = -1$, and $\Omega = [\omega_a, \omega_b]$, $0 \le \omega_a < \omega_b$ – the frequency range of interest that contains the frequencies ω of the controllers. The convergence of the learning process is guaranteed because (5) results in

$$\|e_i\|_\infty \le \gamma^i \|e_0\|_\infty \to 0 \text{ as } i \to \infty. \tag{7}$$

Using the control system structure in Figure 1, the convergence condition can be transformed into

$$\left\| 1 - \frac{P\,C\,C_1}{1 + P\,C} \right\|_\infty \le \gamma < 1. \tag{8}$$

The design approach consists of the following design steps based on frequency domain designs:
Step 1. Carry out a frequency domain design to tune the parameters of the controller with the transfer function C that belongs to the control loop in the

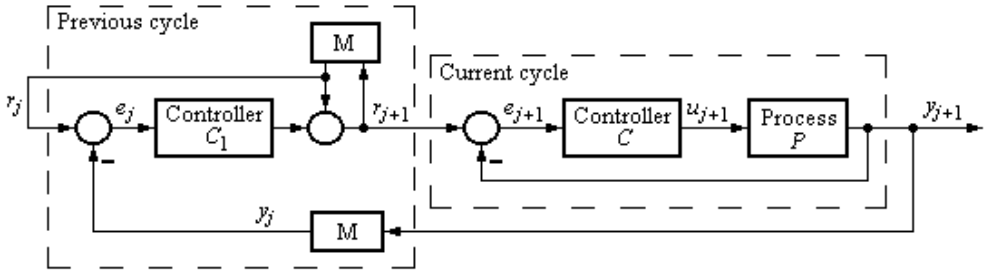

Figure 1: ILC-based control system structure with CL.

current cycle. The value of the phase margin is imposed to ensure not only stable control system in the current cycle that guarantees a finite e_0 but also acceptable performance indices of this control system which is subject to performance improvement by ILC.

Step 2. Set the value of the parameter γ and carry out a frequency domain design that employs (6) to tune the parameters of the controller with the transfer function C_1 that belongs to the control loop in the previous cycle. The parameters of C_1 are tuned such that to fulfil the condition (8).

4 REAL-TIME EXPERIMENTAL RESULTS

Our design approach is tested through experiments on a 3D crane system laboratory equipment (Inteco, 2008) to validate it for the two ILC-based control system structures presented in the previous section. Our experimental setup consists of a rail moving along the frame, a cart moving on the rail, and a payload being shifted up and down.

The ILC-based control system structure controls separately the x-axis and the y-axis, i.e., it controls x_1 and x_3, respectively, using the process transfer functions $P(s) = H_x(s)$ and $P(s) = H_y(s)$, respectively, defined in (3). The two steps of the design approach use the lead-lag controllers and the real PD learning rules with the transfer functions $C(s)$ and $C_1(s)$, respectively:

$$C(s) = k_c \frac{1+T_a s}{1+T_b s},\ C_1(s) = k_1 \frac{1+T_c s}{1+T_d s}, \qquad (9)$$

where k_c and k_1 are gains, and T_a, T_b, T_c and T_d are time constants.

The two steps of the design approach were applied such that to obtain the same parameter values for both processes, i.e., both axis, x and y. This simplification is possible because of the inequality-type convergence condition (8). The frequency domain approaches applied in the two steps of the design approach resulted in the parameter values

$$k_c = 0.1,\ k_1 = 1.5,\ T_a = 1\,\text{s},$$
$$T_b = T_d = 0.01\,\text{s},\ T_c = 0.07\,\text{s}. \qquad (10)$$

A part of the real-time experimental results is presented as follows for reference inputs r_j that characterize an arc of a circle in the (x_1, x_3) plane, referred to also as the xy plane. The results are expressed as the responses of x_1 and x_3 as controlled outputs (i.e., they play the role of y_{j+1} according to Figure 1) after one iteration and after several iterations. The system responses of the ILC-based control system structure with CL are presented in Figure 2. The results prove the strong control system performance improvement with respect to the first cycle (experiment). A good tracking performance is ensured.

5 CONCLUSIONS

This paper has suggested an ILC-based control system structure that involves CL. The combination with PD controllers and learning rules and application to the position control of a 3D crane system laboratory equipment is convenient because this equipment allows the application of repeatable reference inputs and initial conditions over the cycles (iterations) of the ILC learning processes.

Our design approach is important as it ensures the serious improvement of the control system performance indices (overshoot, settling time, etc.) in the system responses with respect to the reference input. However the disturbance rejection is not carried out since we used PD controllers.

Our continuous-time design approach is justified

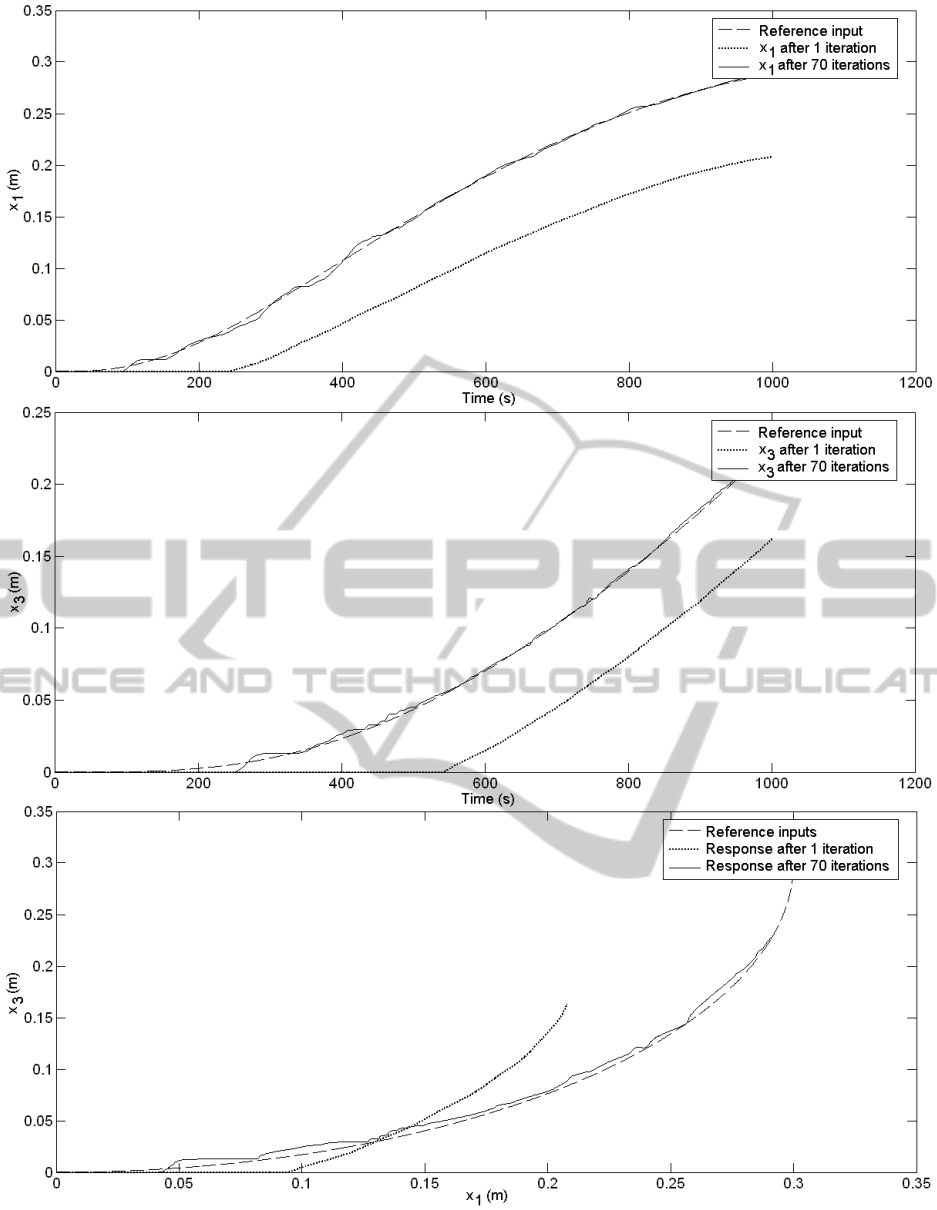

Figure 2: Experimental results: the system responses after 1 and after 70 iterations for the ILC-based control system structure with CL.

because of its simplicity in the design. Therefore it is applicable to other nonlinear processes in various fields (Cottenceau et al., 2001; Horváth and Rudas, 2004; Škrjanc et al., 2005; Johanyák et al., 2006; Bellomo et al., 2008; Bernard and Tichkiewitch, 2008; Derr and Manic, 2008; Vaščák, 2009). The only constraint concerns the repeatability of the inputs and of the initial conditions related to the control systems.

Future research will be focused on the application of our ILC-based control structures to the z-axis crane position control problem and to the anti-swing control problem. The extensions to discrete-time control system structures are aimed.

ACKNOWLEDGEMENTS

This work was partially supported by the UEFISCDI of Romania, and by the strategic grant POSDRU 6/1.5/S/13 (2008) of the Ministry of Labour, Family and Social Protection, Romania, co-financed by the European Social Fund – Investing in People.

REFERENCES

Ahn, H.-S., Moore, K. L., Chen, Y., 2007. Iterative Learning Control. *Robustness and Monotonic Convergence for Interval Systems*. Berlin, Heidelberg, New York: Springer-Verlag.

Bellomo, D., Naso, D., Babuška, R., 2008. Adaptive fuzzy control of a non-linear servo-drive: theory and experimental results. *Engineering Applications of Artificial Intelligence*. 21, 846-857.

Bernard, A., Tichkiewitch, S. (Eds.), 2008. Methods and Tools for Effective Knowledge Life-Cycle-Management. Berlin, Heidelberg, New York: Springer-Verlag.

Bristow, D. A., Tharayil, M., Alleyne, A. G., 2006. A survey of iterative learning control. *IEEE Control Systems Magazine*. 26, 96-114.

Chang, C.-Y., Chiang, K.-H., 2008. The nonlinear 3-D crane control with an intelligent operating method. In *Proceedings of 2008 SICE Annual Conference*. Tokyo, Japan, 2917-2921.

Chen, W., Wu, Q., Tafazzoli, E., Saif, M., 2008. Actuator fault diagnosis using high-order sliding mode differentiator (HOSMD) and its application to a laboratory 3D crane. *In Proceedings of 17th World Congress of the International Federation of Automatic Control*. Seoul, Korea, 4809-4814.

Chwa, D., 2009. Nonlinear tracking control of 3-D overhead cranes against the initial swing angle and the variation of payload weight. *IEEE Transactions on Control Systems Technology*. 17, 876-883.

Cottenceau, B., Hardouin, L., Boimond, J.-L., Ferrier, J.-L., 2001. Model reference control for timed event graphs in dioids. Automatica. 37, 1451-1458.

Cuenca, Á., Salt, J., Sala, A., Piza, R., 2011. A delay-dependent dual-Rate PID controller over an Ethernet network. *IEEE Transactions on Industrial Informatics*. 7, 18-29.

Derr, K., Manic, M., 2008. Wireless based object tracking based on neural networks. *In Proceedings of 3rd IEEE Conference on Industrial Electronics and Applications (ICIEA 2008)*. Singapore, 308-313.

Enache, F.-C., 2010. Iterative learning control-based control solutions. Applications to a 3D crane laboratory equipment. B.Sc. Thesis, Department of Automation and Applied Informatics, "Politehnica" University of Timisoara, Timisoara, Romania.

Horváth, L., Rudas, I. J., 2004. Modeling and Problem Solving Methods for Engineers. Burlington, MA: Academic Press, Elsevier.

Inteco Ltd, 2008. 3D Crane, User's Manual. Krakow, Poland: Inteco Ltd.

Johanyák, Z. C., Tikk, S., Kovács, S., Wong, K. K., 2006. Fuzzy rule interpolation Matlab toolbox - FRI toolbox. *In Proceedings of 15th International Conference on Fuzzy Systems* (FUZZ-IEEE'06). Vancouver, BC, Canada, 1427-1433.

Kaneshige, A., Miyoshi, T., Terashima, K., 2009. The development of an autonomous mobile overhead crane system for the liquid tank transfer. *In Proceedings of 2009 IEEE/ASME International Conference on Advanced Intelligent Mechatronics* (AIM 2009). Singapore, 630-635.

Pisano, A., Scodina, S., Usai, E., 2010. Load swing suppression in the 3-dimensional overhead crane via second-order sliding-modes. *In Proceedings of 11th International Workshop on Variable Structure Systems* (VSS 2010). Mexico City, Mexico, 452-457.

Škrjanc, Blažič S., Agamennoni, O. E., 2005. Identification of dynamical systems with a robust interval fuzzy model. Automatica. 41, 327-332.

Vaščák, J., 2009. Using neural gas networks in traffic navigation. Acta Technica Jaurinensis, Series Intelligentia Computatorica. 2, 203-215.

Westerberg, S., Manchester, I. R., Mettin, U., La Hera, P., Shiriaev, A., 2008. Virtual environment teleoperation of a hydraulic forestry crane. *In Proceedings of 2008 IEEE International Conference on Robotics and Automation* (ICRA 2008). Pasadena, CA, USA, 4049-4054.

Xu, J.-X., Panda, S. K., Lee, T. H., 2009. Real-time Iterative Learning Control. Design and Applications. Berlin, Heidelberg, New York: Springer-Verlag.

Yoshida, Y. Tabata, H., 2008. Visual feedback control of an overhead crane and its combination with time-optimal control. *In Proceedings of 2008 IEEE/ASME International Conference on Advanced Intelligent Mechatronics* (AIM 2008). Xi'an, China, 1114-1119.